An Alkyne Linchpin Strategy for Drug:Pharmacophore Conjugation: Experimental and Computational Realization of a *meta*-selective Inverse Sonogashira Coupling

Sandip Porey,[1,†] Xinglong Zhang,[2,†] Suman Bhowmick,[1] Vikas Kumar Singh,[1] Srimanta Guin,[1,*] Robert S. Paton,[2,3,*] and Debabrata Maiti[1,4,*]

[1]Department of Chemistry, Indian Institute of Technology Bombay, Powai, Mumbai 400076, India

[2]Chemistry Research Laboratory, University of Oxford, Mansfield Road, Oxford, OX1 3TA, UK

[3]Department of Chemistry, Colorado State University, Fort Collins, Colorado 80523, USA

[4]Tokyo Tech World Research Hub Initiative (WRHI), Laboratory for Chemistry and Life Science, Tokyo Institute of Technology, Japan

[†]These authors contributed equally to this work

Email: dmaiti@iitb.ac.in (DM)
Email: robert.paton@colostate.edu (RSP)
Email: srgnchem@gmail.com (SG)

Abstract

The late-stage functionalization (LSF) of pharmaceutical and agrochemical compounds by the site-selective activation of C–H bonds offers immediate access to diverse structural analogs and expands the accessible chemical space. We report a C–H functionalization LSF strategy that hinges on the use of an alkyne linchpin to assemble conjugates of sp^2-rich marketed pharmaceuticals and agrochemicals with sp^3-rich 3D-fragments and natural products. This is accomplished through a template-assisted inverse Sonogashira reaction that displays high levels of selectivity for the *meta*-position. This protocol is also amenable to distal structural modifications of α-amino acids. The transformation of alkyne functionality to other functional groups further highlights the applicative potential. Computational and experimental mechanistic studies shed light on the detailed mechanism. Turnover-limiting 1,2-migratory insertion of the bromoalkyne

coupling partner occurs after relatively fast C–H activation. While this insertion occurs unselectively, regioconvergence results from one of the adducts undergoing a 1,2-trialkylsilyl migration to form the alkynylated product. A heterobimetallic Pd–Ag TS, which is essential for product formation, is explicitly implicated in the *β*-bromide elimination step.

1. Introduction

The direct functionalization of unactivated C–H bonds continues to challenge chemists and inspire new chemistry.[1] As the synthetic toolbox of C–H functionalization reactions continues to grow, concerted effort has focused on harnessing broad functional group compatibility to accommodate the demands of complex molecule synthesis.[2] For medicinal chemistry, emerging C–H functionalization methods present opportunities to explore chemical space inaccessible by conventional synthetic processes.[3] The recognition of C–H bonds as sites for potential diversification expands the availability of late-stage functionalization (LSF) strategies and enables the development and diversification of biologically active molecules without resorting to *de novo* synthesis.[4] Furthermore, LSF facilitates the exploration of structure-activity relationships, the optimization of physical properties, and enables new reaction vectors to be explored. However, a major challenge towards the widespread adoption of LSF by C–H bond functionalization of pharmaceutical compounds is the requirement for precise control over site-selectivity: This challenge is compounded by the abundance of heteroatoms in drug like fragments,[5] as these Lewis basic sites bind competitively with catalysts, resulting in potentially undesirable site-selectivity or catalyst poisoning.[6]

Significant advances in the selective post-synthetic modification of pharmaceutical compounds have been accomplished by chelation assisted *ortho*-functionalization.[4,7] In contrast, *meta* and *para*

C(sp^2)–H functionalizations[8] are less well-developed for this purpose. Strategic access to alternative regioisomers *via* site-selective C–H functionalization would provide an entry to alternative spatial arrangements of medicinally-important functionalities and an expanded chemical space.[9] The same logic holds true for the structural diversification of α-amino acids, which forms the basis of various bioactive oligopeptides.[10] We were therefore intrigued by the prospect of developing LSF protocols harnessing *meta* C(sp^2)–H functionalization and a subsequent alkynylation reaction *via* an inverse Sonogashira cross-coupling with haloalkynes.[11] The alkyne functionality provides a rigid and versatile spacer group that permits broad exploration of chemical space through LSF.[12] For example, an acetylene group can be covalently linked to ketones by a simple nucleophilic addition, such that carbonyl-containing sp^3-rich natural product fragments can be conjugated to (hetero)aromatic fragments (Figure 1). Through this coupling reaction, a wide range of pharmaceutically relevant ketones, including biologically active compounds *e.g.* estradiol or natural products *e.g.* menthol, could be covalently attached to various drug-molecules. This transformation also provides direct access to structural modifications of α-amino acids such as phenylalanine and tryptophan. However, state-of-the-art protocols for C(sp^2)–H alkynylation are currently restricted to a narrow range of alkyne variants, with silyl acetylenic derivatives displaying unique reactivity as coupling partners.[13-15] The exploration of broader alkyne scope is therefore an essential step in developing a *meta*-selective conjugation protocol of aromatic drugs with 3D-pharmacophores. To the best of our knowledge, this protocol represents the first of its kind to access drug-pharmacophore conjugates by an inverse Sonogashira reaction, which occurs selectively at the *meta*-position of arenes.

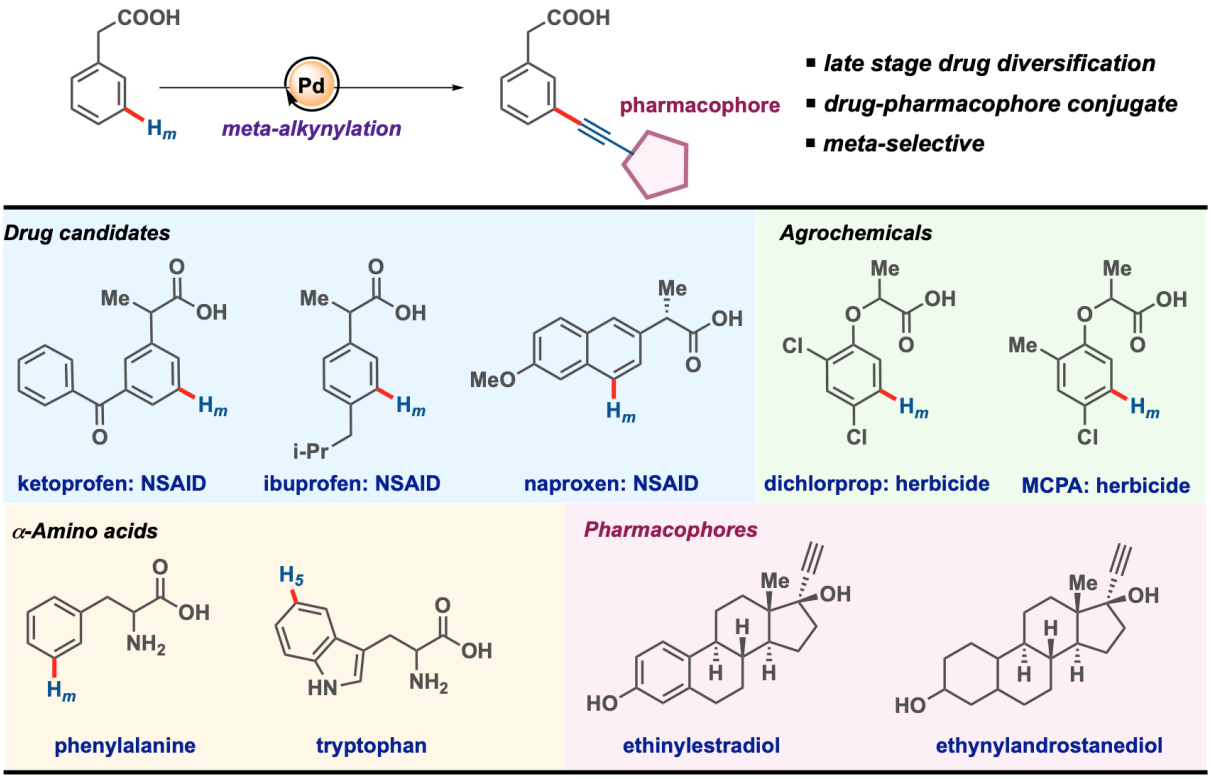

Figure 1. Linchpin Approach for Diversification through the Conjugation of sp^2-Rich Aromatic and 3D Fragments

2. Results and Discussion

Optimization of reaction parameters. The inverse Sonogashira coupling of 3-methyl substituted benzyl sulfonate ester **1a** with triisopropylsilyl acetylene bromide **1b** was explored to optimize reaction parameters. A pyrimidine based *meta*-directing group (DG) was employed due to its efficacy as a strong σ-donating and π-accepting ligand, contributing to its success in accomplishing different functionalizations.[16] An oxidant such as a silver salt is required to regenerate the active Pd catalyst after each catalytic cycle.[17] Accordingly, *m*-alkynylation was carried out with $Pd(OAc)_2$ as catalyst in the presence of *N*-Ac-Gly ligand and AgOAc oxidant. Hexafluoroisopropanol (HFIP) solvent has been used previously to promote distal C(sp^2)–H

functionalization, however, we observed no reactivity under these conditions.[18] In contrast, with a fluorinated aprotic solvent, benzotrifluoride, formation of the desired *m*-alkynylated product **1** was observed, in poor yield but with excellent selectivity. Persisting with benzotrifluoride as solvent, systematic alterations of different reaction parameters showed that AgOAc and $Cu(OAc)_2$ were both essential. Gratifyingly, the yield of the *m*-alkynylated product could be further increased switching to 1,4-dioxane as solvent. Pyridine, quinoline and nitrile based *meta* DGs (**DG_2-DG_8**, Table 1) were inferior to pyrimidine (**DG_1**, Table 1). Full details of these optimization studies are provided in Supporting Information (see SI 2.2.a).

Table 1. Evaluation of Directing Groups

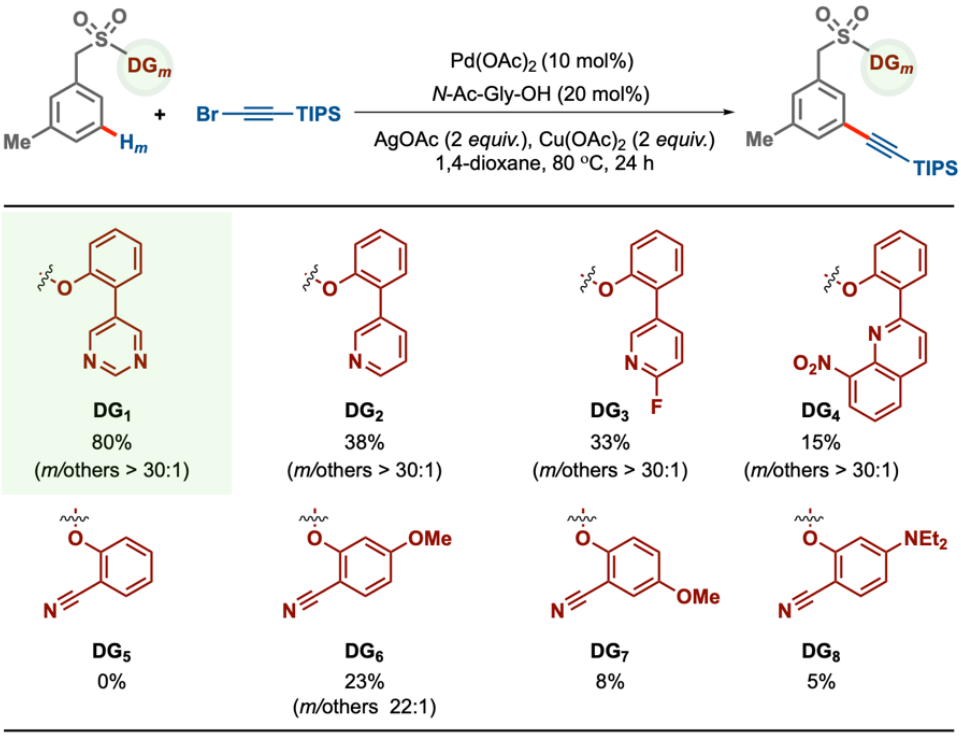

Scope of *meta*-selective C–H alkynylation. The optimized reaction conditions were used to explore reaction scope. Strikingly, *meta*-selective C–H alkynylation tolerates benzyl sulfonyl esters with electronically diverse aromatic substituents in *ortho*, *meta* and *para* positions. The

anticipated alkynylated products were obtained in synthetically useful yields along with excellent *meta*-selectivity (Scheme 1). More importantly, reactive chloro- (**9**), bromo- (**3**), acetoxy (**6**) and ester (**7**) functional groups were left untouched, while a thiophene moiety at the *meta*-position (**15**) was also a viable substrate. Variation of the alkyl group connecting the DG was then explored (Scheme 2). Substituted and unsubstituted arenes with ethyl, propyl, butyl chains provided exclusively mono-alkynylated products in good yields and selectivity (**17**-**23**). It is noteworthy that the *meta*-selectivity decreases with increasing chain length of the directing group (**17**-**19**, Scheme 2), indicating a diminishing *meta*-selectivity control *via* ring strain, as we would predict from our computational modelling showing that *meta*-selectivity is controlled predominantly by steric strains of the cyclopalladated insertion TS structure (*vide infra*; DFT studies in SI 2.6.15).

Scheme 1. Scope of the Reaction with Benzylsulfonyl Esters[a]

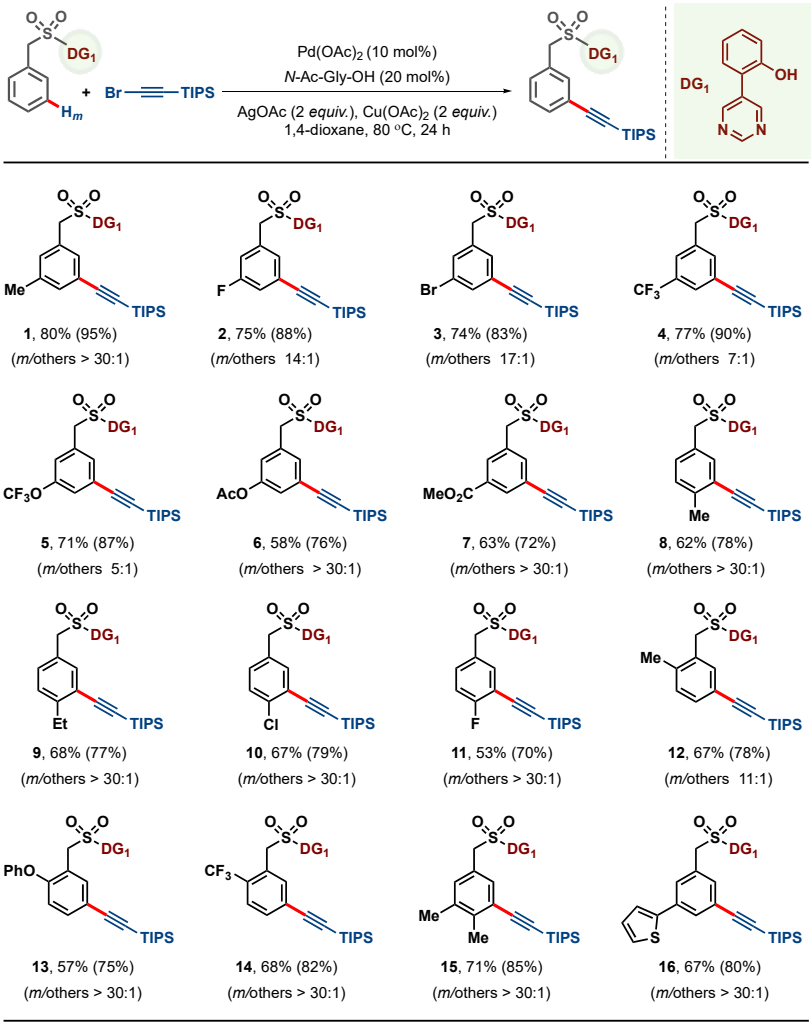

[a]Yield in parenthesis is based on unreacted starting material.

The robustness of the protocol was demonstrated using phenyl acetic acids and benzyl silyl ethers as substrates (Scheme 2). In all cases, a range of substituents with varying electronic and steric properties were compatible (**24**-**43**). Arenes possessing methoxy group gave useful yields of their corresponding *m*-alkynylated products with high regioselectivity (**20**, **22**, **27**, **31**, **32**, **40** and **43**, Scheme 2). Phenyl (**34**) and cyclopropyl (**35**) groups were well tolerated at the α-position of phenylacetic acids. Intriguingly, the present protocol provides an

Scheme 2. Scope of the Reaction with Variable Chain-length Tethered Scaffolds, Phenylacetic Acids and Benzylsilyl Ethers[a]

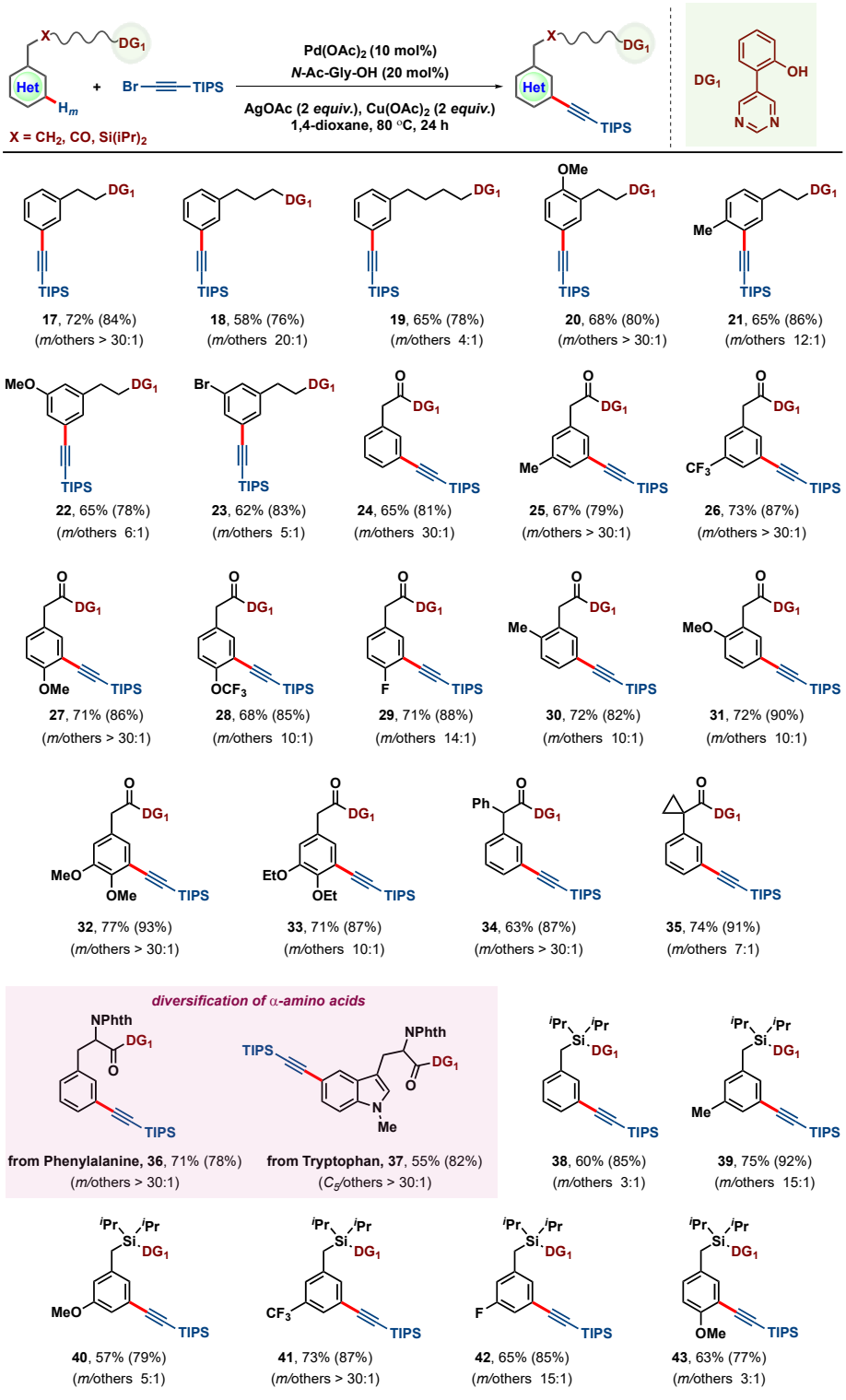

[a]Yield in parenthesis is based on unreacted starting material.

access to diversified unnatural amino acids. *Meta*-selective alkynylated product **36** was obtained from the phenylalanine derivative in high yield and selectivity, while C5 alkynylation of the tryptophan derivative gave **37** in excellent selectivity. To the best of our knowledge, this constitutes the first example of an indole alkylation at the distal C5 position by directed C–H activation.

We next investigated generality with respect to the alkyne (Scheme 3). Propargyl silyl ethers prepared by nucleophilic addition to a series of ketones were reacted with arenes with different linker systems. The alkynyl bromide derived from menthone (itself of pharmaceutical relevance) underwent facile reaction with different scaffolds in good yields and selectivities (**44**, **46**, **51**, **53-56**). Similarly, *meta*-alkynylation carried out with alkynyl bromides obtained from the bicyclic ketone, 2-norbornanone (**45 and 50**), cyclohexanone derivative (**48**) and larger ring system cyclooctanone (**49**) proceeded smoothly to provide synthetically useful yields of their corresponding products. Notably, a phenol derivative was a competent substrate, providing *meta*-selective product **46**, the DG overcoming any innate electronic bias towards *ortho* functionalization. Androstanediol, a potent $GABA_A$ receptor,[19] could also be conjugated selectively at the *meta* position (**52**), regardless of the steric hindrance exerted by the bulky steroid. The (protected) diol product contains the ethynylandrostanediol fragment, an orally active analogue of 17-substituted androstanediol used to treat cancer. When phenyl acetylenic bromide was used as the alkynylating agent, the reaction failed to proceed. The same observation was noted with triisopropylsilyl acetylene also. The incompatibility of these substrates was subsequently rationalized computationally (see Supporting Information, section 2.6.10 and SI 2.6.11). Noteworthy, while most substrates gave high *meta*-selectivity, for others the level of selectivity

was moderate. The origin for these differences in selectivity (even using the same DG) lies in the conformation of transition states of the metal complex, which in turn are governed by the stereo-electronic factors and steric hindrance in solution state. Perturbations from the ideal conformation for *meta*-functionalization lead to the formation of other isomers and reduce regioselectivity. An in-depth analysis for quantitative determination of selectivity with variation in substituents by computational methods is currently underway in our laboratory (see supporting information, section SI 2.6.14 and SI 2.6.15 for further details).

Scheme 3. Scope of the reaction with alkyne variants[a]

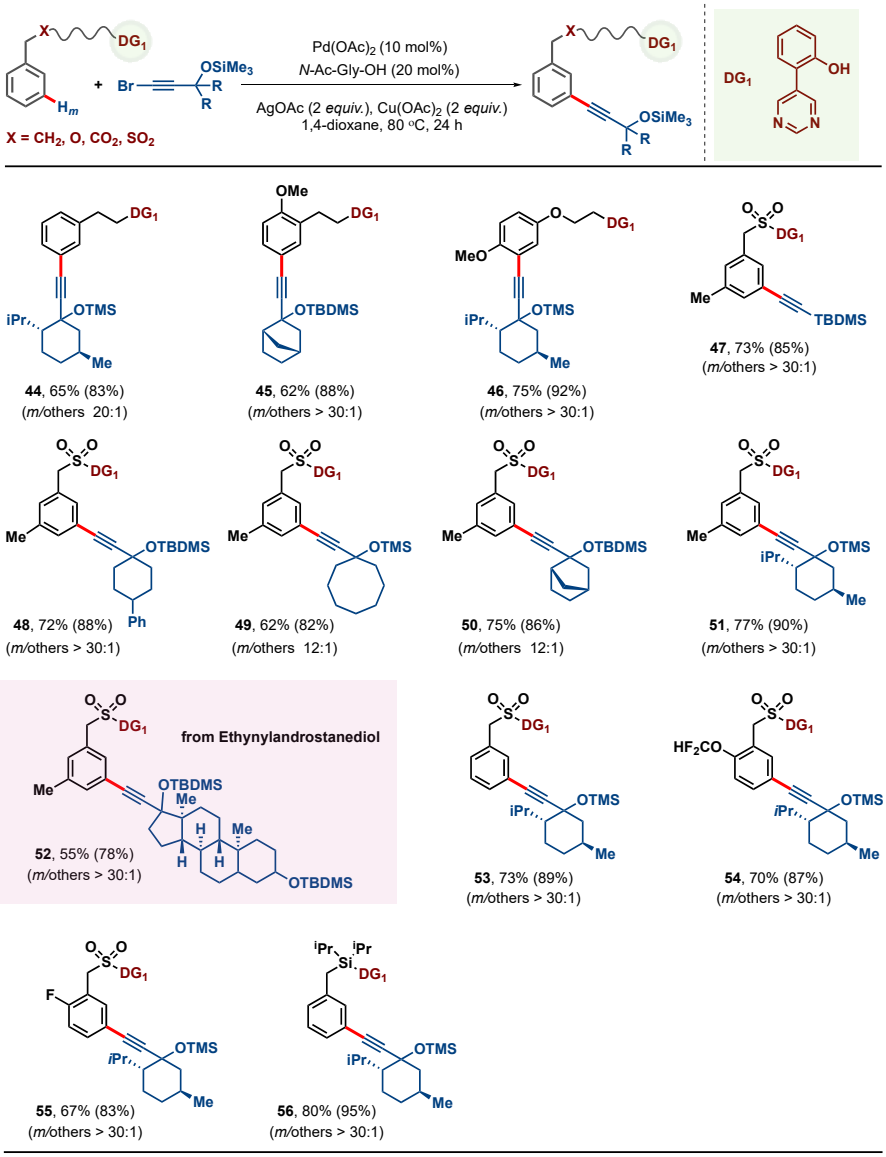

[a]Yield in parenthesis is based on unreacted starting material.

Pharmaceutical and agrochemical LSF was then examined using this newly developed protocol (Scheme 4a). To this aim, marketed nonsteroidal anti-inflammatory drugs such as ketoprofen (**57**), ibuprofen (**58**), naproxen (**59**), baclophen (**63**) were transformed to their *m*-alkynylated derivatives in excellent selectivity with triisopropylsilyl acetylene bromide. Phenoxy based agrochemicals and drugs such as dichlorprop (herbicide, **60**), clofibric acid (lipid lowering agent, **61**) and MCPA (herbicide, **62**) were similarly functionalized.

Scheme 4. Late-stage functionalization of drugs and agrochemicals[a]

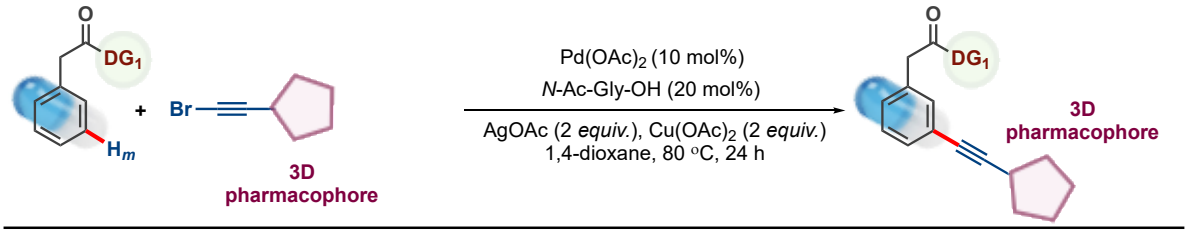

a ***Late-stage diversification of drug molecules***

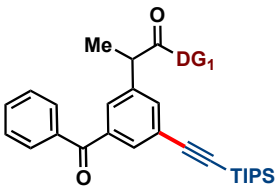

57, 82% (91%)
(*meta* exclusive)
from ketoprofen: NSAID

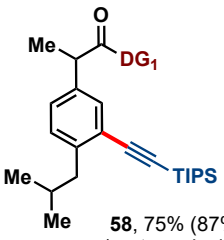

58, 75% (87%)
(*meta* exclusive)
from ibuprofen: NSAID

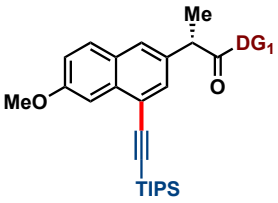

59, 72% (82%)
(*meta* exclusive)
from naproxen: NSAID

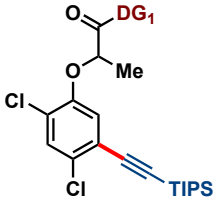

60, 75% (85%)
(*meta* exclusive)
from dichlorprop: herbicide

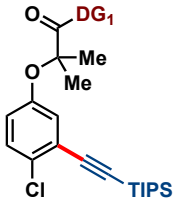

61, 77% (87%)
(*meta* exclusive)
from clorfibric acid: lipid lowering

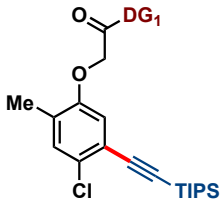

62, 79% (88%)
(*meta* exclusive)
from MCPA: herbicide

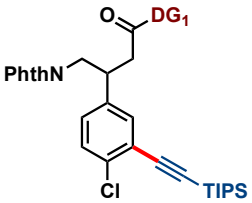

63, 66% (76%)
(*meta* exclusive)
from baclophen: NSAID

b ***Drug-3D fragment conjugate***

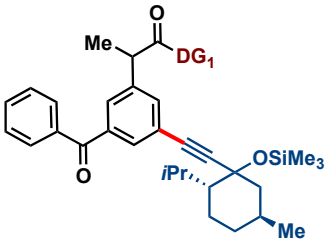

64, 82% (92%) (*meta* exclusive)
ketoprofen-menthol conjugate
menthol: anesthetic

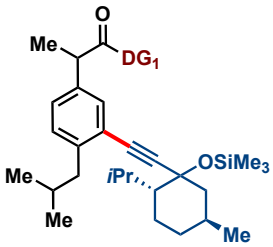

65, 77% (93%) (*meta* exclusive)
ibuprofen-menthol conjugate
menthol: anesthetic

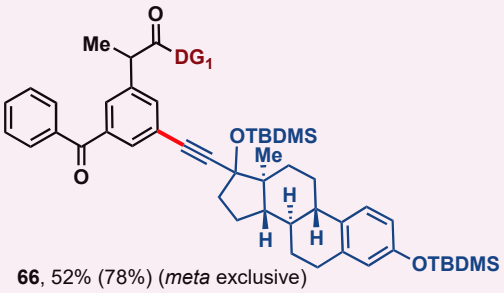

66, 52% (78%) (*meta* exclusive)
ketoprofen-estradiol conjugate
estradiol: estrogen receptor

[a]Yield in parenthesis is based on unreacted starting material.

Further structural diversification of marketed sp^2-rich aromatic drugs was achieved through conjugation with sp^3-rich 3D-fragments (Scheme 4b). Both ketoprofen and ibuprofen afforded

meta-products conjugated with menthol in excellent yields and *m*-selectivity (**64** and **65**). Ethinylestradiol, an orally active derivative of estradiol used as estrogen medication,[20] could selectively be introduced to the *meta*-position of ketoprofen (**66**) in preparatively useful yield. The conjugation with aliphatic fragments provides access to an expanded chemical space, escaping the "flatland" of aromatic drugs. In principle, this approach could be used to modulate the bioactivity of either parent molecule.

Applications of *meta*-alkynylation protocol. Iterative functionalization at both *meta*-positions of a benzyl sulfonate ester provides access to further molecular complexity. This sequential process could be carried out with olefination, alkylation and cyanation following reported procedures. The mono-functionalized products underwent alkynylation at vacant *meta* position to provide heterodifunctionalized products **67**-**69** (Scheme 5). Two different alkynes could also be introduced iteratively (**70**). The iterative *m*,*m*'-difunctionalizations were also applicable for other tethering scaffolds (**71**-**76**, Scheme 5). The synthetic utility was further demonstrated by conducting a gram scale reaction that provided an acceptable yield of the product (Scheme 6a). Removal of the directing group for carbonyl scaffold (**30**) under mild conditions affords the parent acid **77**. While for the silyl scaffold (**38**), treatment with tetrabutylammonium fluoride (TBAF) gives the corresponding silanol (**78**) without affecting the alkyne part (Scheme 6b). In both cases, the directing group could be recovered in high yields, demonstrating the practicality of this protocol. Finally, the *meta*-alkynylated benzyl sulfonate ester could be transformed into other functional groups (Scheme 6c). A Julia olefination reaction of **1** led to the formation of olefinated product **80** along with concomitant removal of sulfonate group. A ruthenium catalyzed oxidation of **1** gave the corresponding *meta*-carboxylic acid **81** by C–C bond cleavage while treatment with formic

acid under reflux condition afforded the *meta*-acyl product **82**. Furthermore, CsF enabled desilylation followed by copper catalyzed click reaction with tosylazide gave the *meta*-triazole product **83**.

Scheme 5. Sequential Heterodifunctionalization

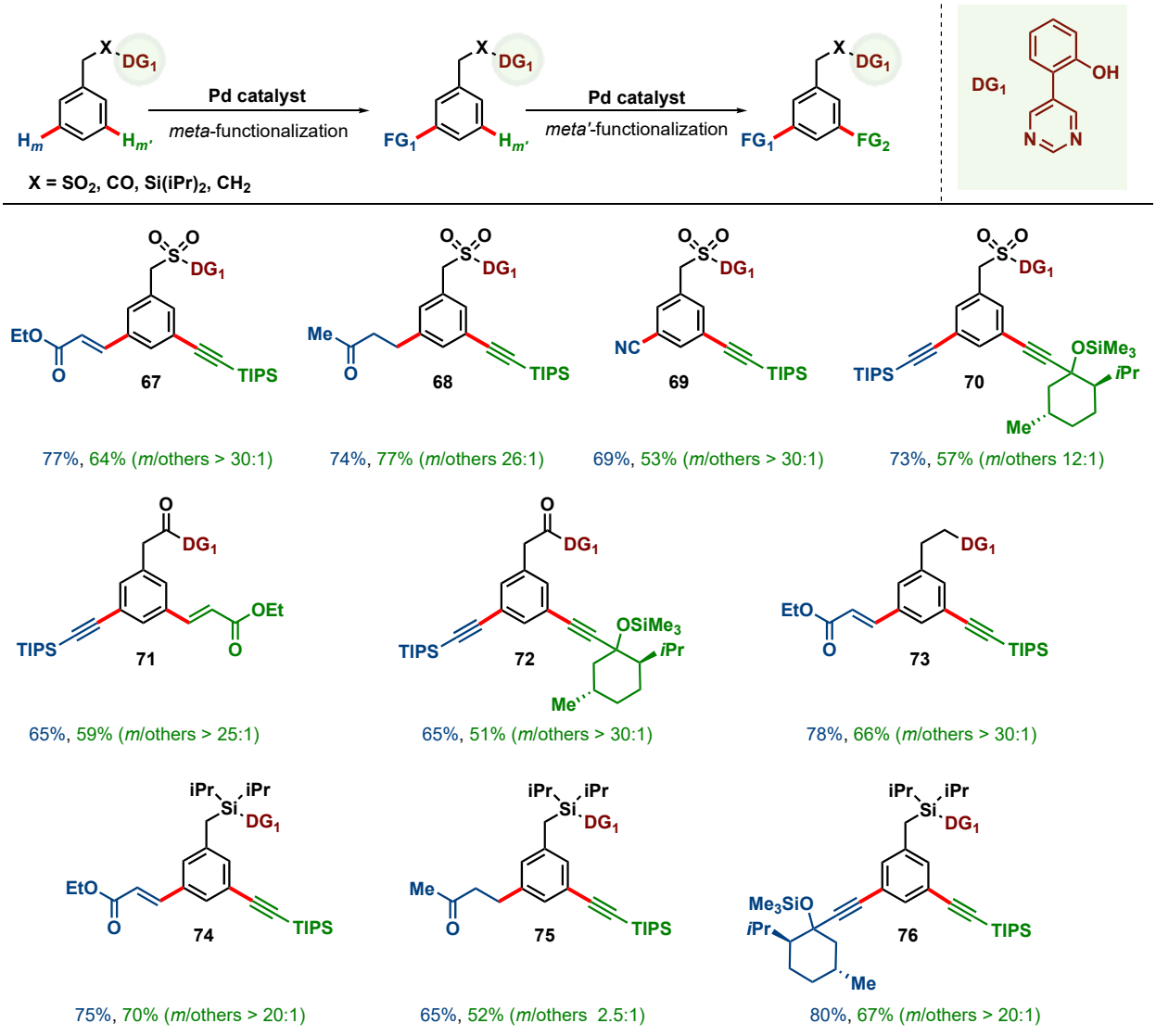

Scheme 6. Applicative Potential of *meta* C–H Alkynylation

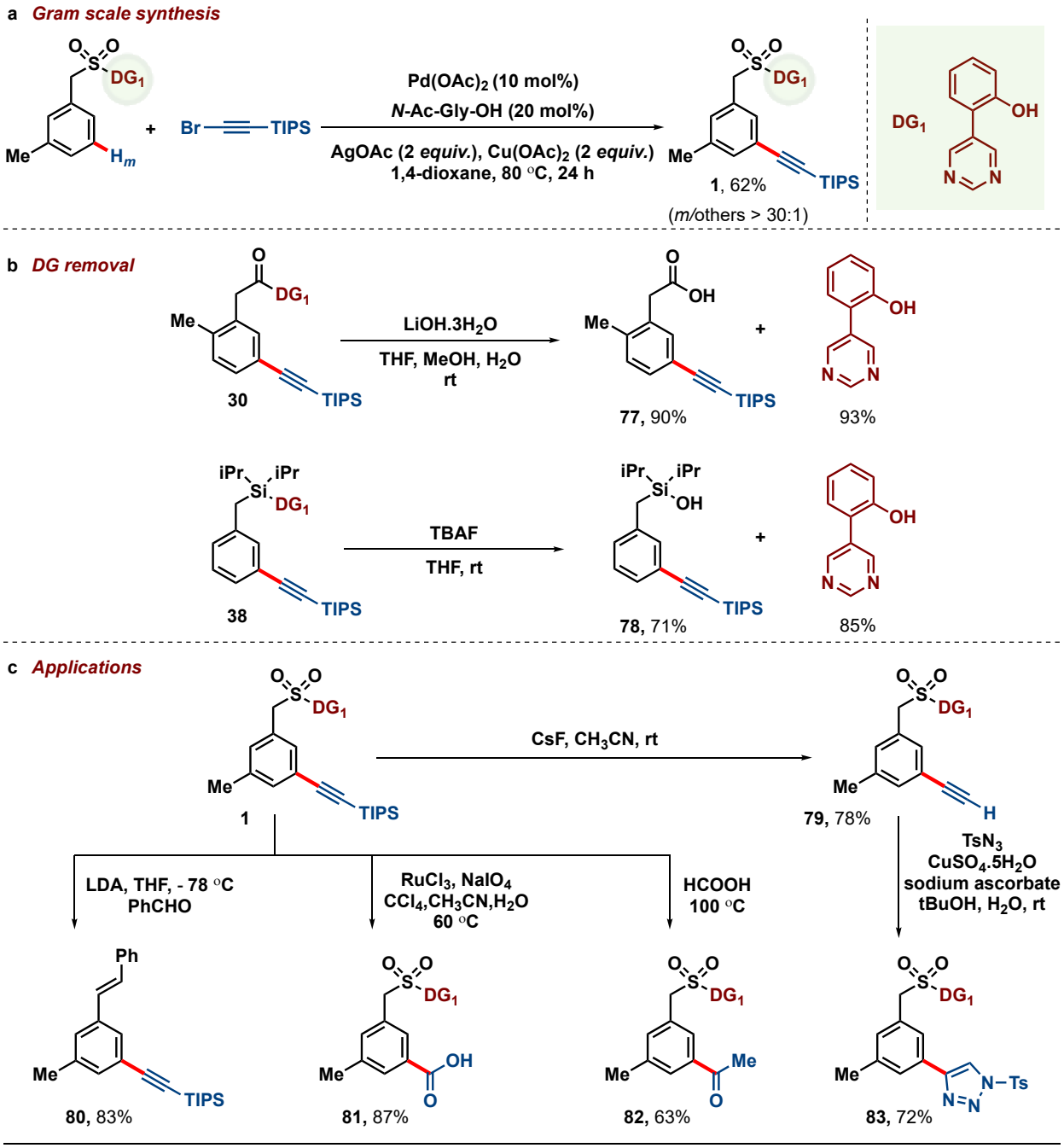

3. Mechanistic Investigation and Computational Studies

Kinetic experiments and computational studies were performed to investigate the reaction mechanism. Kinetic isotope effect (KIE) studies performed with **1a** and its deuterated analogue **1a-*D*** (parallel experiments) gave a value close to unity ($k_H/k_D = 1.04$) implying C–H scission does not occur in the turnover determining transition state (TDTS) of the catalytic cycle (Scheme 7a). The importance of ligand in lowering the activation barrier for C-H activation step as well as achieving a better *meta* selectivity was adjudged by performing a series of control reactions. In absence of ligand, the reaction under standard conditions provided the alkynylated product in poor yield and selectivity (17%, *m*:others 2:1). Alkynylation at higher temperatures (100 and 120 °C) provided only a slight enhancement in yield but no improvement in selectivity (see SI 2.5). A similar reaction carried out with the deuterated analogue **1a-D** gave a significantly lower yield (5%) of the desired product. These data are consistent with C-H activation becoming rate-determining without an *N*-protected amino acid. Furthermore, a first order dependence with respect to substrate, alkyne and ligand was observed (Scheme 7b), implicating their involvement in or prior to the TDTS (see SI 2.5).

Scheme 7. Mechanistic Investigation of Palladium Catalyzed *meta* C–H Alkynylation

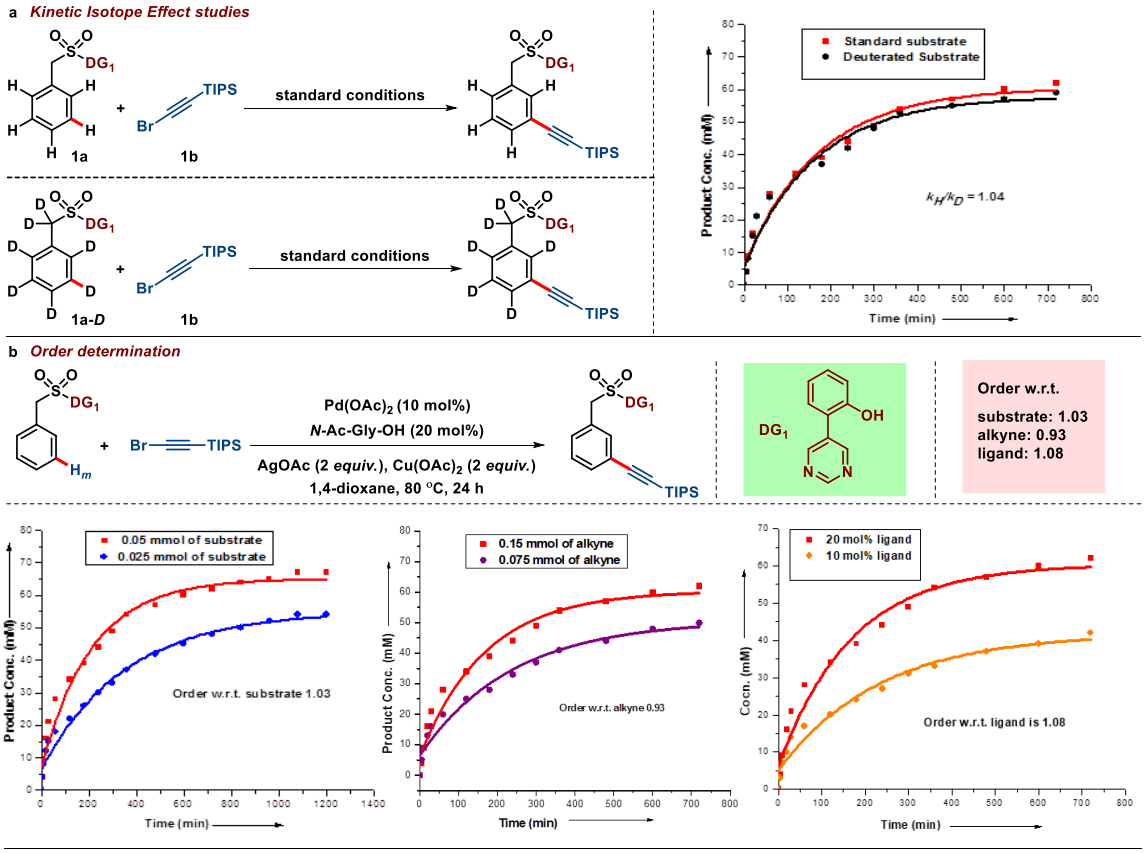

Density functional theory (DFT) calculations were used to rationalize the above observations, and to gain insight into events occurring after the TDTS that do not appear in the experimentally determined rate law. Arene **1a** and bromoethynyltrimethylsilane **1b** (hereafter bromoalkyne) were considered in these calculations. Gibbs energy profiles were computed at the SMD (1,4-dioxane)-ωB97X-D(MN15)/def2-QZVPP//MN15/GENECP (def2-TZVPPD for Br, Pd and Ag + def2-SVP for others) level of theory. For geometry optimizations a mixed basis set was used (see SI section 2.6 for full details).[21] An abridged Gibbs energy profile showing a full turn of the catalytic cycle is depicted in Figure 2.

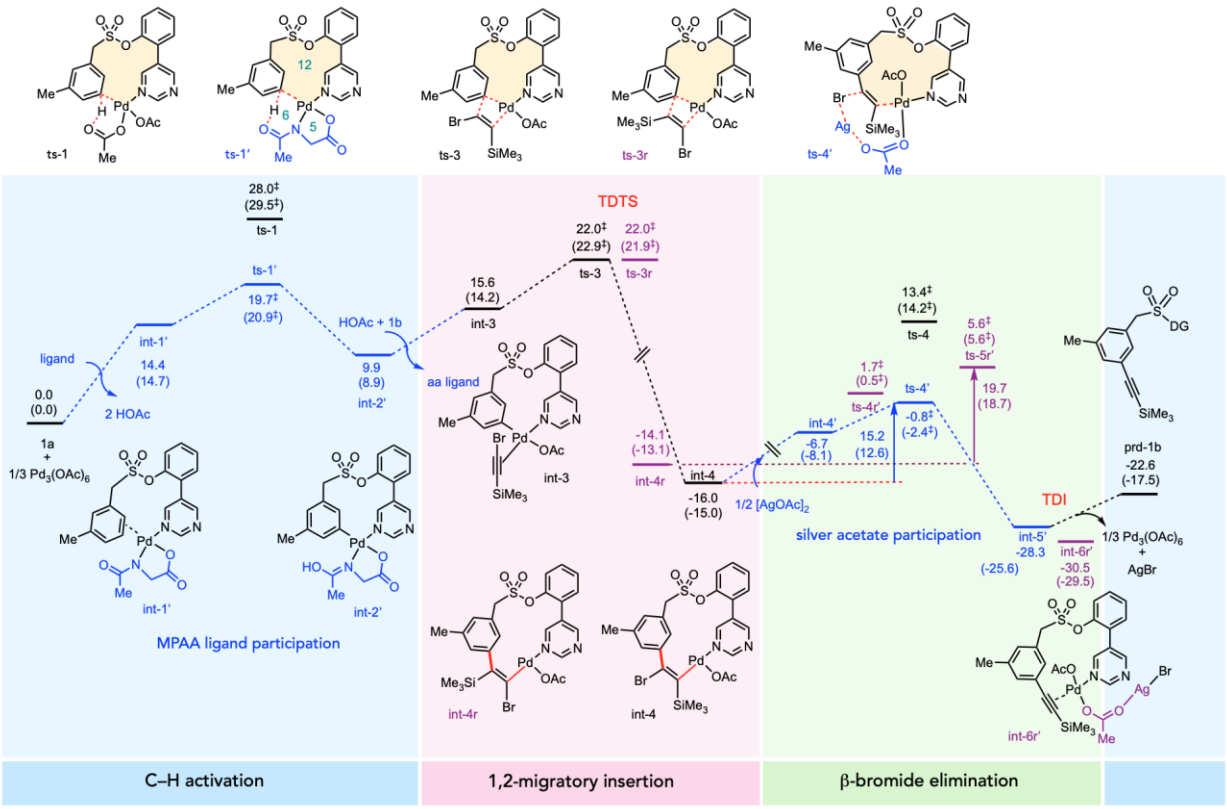

Figure 2. DFT Studies of Palladium Catalyzed *meta* C–H Alkynylation

Computed C–H activation transition structures (TSs) show a kinetic preference for activation of the *meta* C–H bond (see SI 2.6.9), by a factor of 41:1 over the *para* position, and ~8000:1 over the *ortho* position. Without a monoprotected amino acid (MPAA) ligand, C–H activation has a high activation barrier (**ts-1**, 28.0 kcal mol^{-1}), whereas with MPAA *N*-acetylglycine, **ts-1'**contains a [5,6]-palladacycle conducive for C–H activation,[16c,22-25] lowering the barrier of this step to 19.7 kcal mol^{-1}. The amide oxygen is strategically positioned for C–H activation *via* Ambiphilic Metal–Ligand Activation/Concerted Metalation–Deprotonation (AMLA/CMD). Alternative ligand arrangements are uncompetitive (see SI 2.6.3). With the MPAA ligand, C–H activation is computed to proceed reversibly before the TDTS, in agreement with the absence of an experimental primary KIE (measured k_H/k_D = 1.04).

1,2-Migratory insertion of bromoalkyne **1b** is computed to occur in the turnover frequency-determining transition state (TDTS),[26] with a barrier of 22.0 kcal mol^{-1}. This step is also the regio-determining step (*meta*- over *ortho*- or *para*-site) for the overall reaction. Our model suggests strong steric control exerted *via* the ring size in this step (*meta*: 12-membered *vs ortho*: 11-membered *vs para*: 13-membered palladacycle for our prototypical DG_1). This regioselectivity is general for a number of substrates using the same DG with varying electronic factors on the arene substrate (products **4**, **5** and **12**; SI 2.6.14). We attribute site-selectivity to the differing ring strains in the palladacyclic TS, that is minimized in the meta-product. Indeed, we have computed the macrocyclic ring-strain in ortho-, meta- and para- structures relative to an unstrained system using a pyridyl ligand using isodesmic reaction energies (Scheme S4) to quantify this: strain in the meta-TS is lower than the para- and ortho- structures by more than 3 and 5 kcal/mol, respectively. Furthermore, we predict that as the length of the directing group increases the meta site-selectivity will diminish. Indeed, this is what was observed experimentally for products **17**, **18** and **19**, and this is reproduced by our calculations of the competing stabilities of the 1,2-insertion step for these substrates. (DFT studies in SI 2.6.15).

The resting state in the computed catalytic cycle, the turnover determining intermediate (TDI) is the catalyst bound product. Substrate and bromoalkyne both enter the catalytic cycle after this species, consistent with the first order dependence of the rate law on these species' concentrations (Scheme 7b). The calculations also suggest first order dependence on [MPAA] and inverse first order dependence on [product]. The observations from computational studies are in good agreement with the experimental results (Scheme 7b, see SI 2.5). The overall energetic span of the catalytic cycle is 29.9 kcal mol^{-1}, within 2 kcal/mol of that expected for a reaction taking place over 24 h at 80 °C.

The alternative mechanism of oxidative addition of **1c** (see SI 2.6.5) breaking the C(*sp*)–Br σ-bond is uncompetitive at 42.5 kcal mol^{-1}. Migratory insertion is highly exergonic, giving **int-4** at −16.0 kcal mol^{-1}. Subsequent β-bromide elimination, in the absence of silver acetate, has a high activation barrier *via* **ts-4** of 29.4 kcal mol^{-1}; this is lowered to 15.2 kcal mol^{-1} in its presence, *via* a Pd(II)–Ag(I) heterobimetallic TS (**ts-4'**) shown in Fig. 3.[27-29] assisted by the enthalpically favourable formation of insoluble AgBr salt (see SI 2.6.7 for a detailed discussion of the role of the silver acetate additive). Product formation is also favourably exergonic, at −28.3 kcal mol^{-1},with respect to the starting materials.

The migratory insertion step was found to proceed irreversibly with little to no regioselectivity for the present substrate TMS-bromoalkyne (**ts-3** and **ts-3r**, Fig. 2). In accord with observations made by Musaev and Sarpong, Int4 benefits from the antiperiplanar arrangement of donor σ(Pd-C) and acceptor σ*(C-Br) orbitals, resulting in a favorable hyperconjugative interaction that stabilizes this intermediate relative to int4r.[30] From **int-4**, β-elimination occurs forming the silylalkyne *via* the *anti*-periplanar TS, **ts-4'**. On the other hand, the regioisomeric adduct **int-4r**, undergoes a stepwise loss of bromide (**ts-4r'**, at 1.7 kcal mol^{-1}; $\Delta\Delta G^{\ddagger}$ = 14.1 kcal mol^{-1}) and subsequent 1,2-silyl migration (**ts-5r'**, at 5.6 kcal mol^{-1}; $\Delta\Delta G^{\ddagger}$ = 19.7 kcal mol^{-1}) to form the sole silylalkyne product. This 1,2-shift occurs as the Br atom leaves (Figure 3), gaining negative charge (NBO charge goes from +0.106 in **int-4r** and +0.045 in **int-4r'** to -0.312 in **ts-4r'**,-0.501 in **int-5r'** and -0.601 in **ts-5r'**), while its α-carbon gains carbocationic character (NBO charge goes from -0.157 in **int-4r** and -0.151 in **int-4r'** to +0.025 in **ts- 4r'** and +0.097 in **int-5r'**) (SI 2.6.8); similar cationic 1,2-trialkylsilyl migrations have been observed in Ti,[31] Rh,[32] and Au[33,34] catalysis. Analogous anionic 1,*n*-silyl migration has also been observed in organocopper catalysis, although not previously involving Pd-catalysis.[35-37] The barrier for 1,2-silyl migration **ts-5r'** after the insertion step is lower

than the TDTS (**ts-3r**) at 22.0 kcal mol^{-1} and can thus occur efficiently without affecting the overall rate. For other bulkier trialkylsilyl substrates (TIPS-bromoalkyne, Figures S20-21; TBDMS-bromoalkyne, Figures S22-23 and TES-bromoalkyne, Figures S24-25, SI 2.6.13), calculated insertion barriers indicate that steric effects favor the bulkier trialkylsilyl groups *beta* to the forming C-C bond.[30] This is perhaps also the origin of regioselective insertion in silyloxy-substituted alkynyl bromide (Figure S26). Interestingly, however, we found that for all the trialkylsilyl substrates studied, the subsequent 1,2-silyl migration has a lower barrier then the preceding insertion step and is able to convert the minor regioisomer to the silylalkyne product.

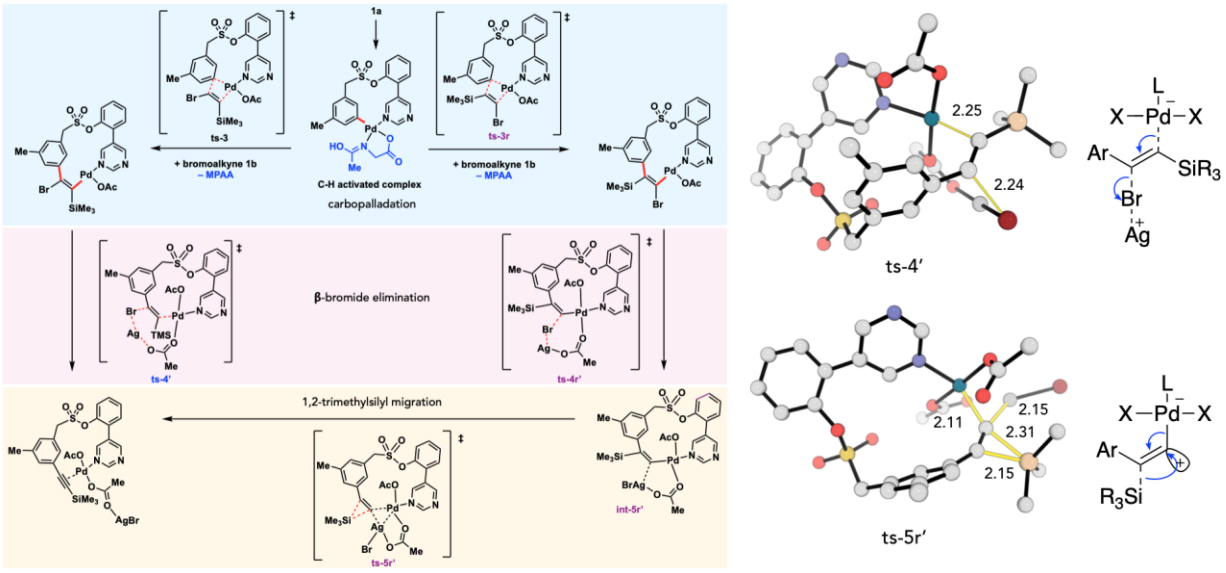

Figure 3. Regioconvergence of C–C Bond Formation

It is noteworthy palladium remains in a formal Pd(II) oxidation state throughout the catalytic cycle, as opposed to a Pd(II)/Pd(IV) manifold. The role of copper(II) acetate was explored computationally (SI 2.6.12). We found that the Pd(II)–Cu(II) heterobimetallic TS (**ts-4'-Cu**, 7.3 kcal mol^{-1}, Fig. S17b) gives an overall barrier of 23.3 kcal mol^{-1}, 8.1 kcal mol^{-1} higher than the Pd(II)–Ag(I) heterobimetallic TS (**ts-4'**, –0.8 kcal mol^{-1}). The Pd(II)–Cu(II) heterobimetallic TS for the regioisomeric rate-determining silyl group migration (**ts-5r'-Cu**, 27.9 kcal mol^{-1}) also has

a higher barrier than the Pd(II)–Ag(I) heterobimetallic TS (**ts-5r'**, 5.6 kcal mol^{-1}). Coordination to the product releases the palladium catalyst for the next cycle. This transmetalation is more thermodynamically favourable than the direct release of product from **int-5'** (Fig. S19), suggesting that it could aid catalyst turnover after each cycle. The reduced copper co-oxidant, Cu(I), could lower the activation barrier of the *β*-bromide elimination (**ts-4'-Cu-I**, –2.7 kcal mol^{-1}, Fig. S17), potentially contributing to an enhanced yield.

4. Conclusions

In summary, we have developed a strategy for *meta*-selective C–H alkynylation in which the alkyne plays a linchpin role coupling sp^2 and sp^3-rich fragments. A diverse variety of substrates including benzyl sulfonate esters, phenyl acetic acids, benzyl silyl ethers and elongated alkyl ethers can be conjugated with aliphatic fragments. This transformation enables site-selective late stage functionalization of *α*-amino acids, marketed drugs and agrochemicals with the addition of bioactive 3D-fragments and natural products. It is also possible to convert the alkyne functionality to other functional groups. Mechanistic investigations suggest that the present Pd-catalyzed *meta*-selective C(sp^2)–H alkynylation proceeds *via* 1,2-migratory insertion, followed by *β*-bromide elimination rather than commonly observed oxidative addition/reductive elimination reaction mode. 1,2-Migratory insertion was found to be the overall turnover limiting transition state, which occurs after relatively rapid and reversible *meta* C–H activation, in agreement with experimental kinetic isotope effects and the measured rate law. 1,2-Migratory insertion occurs irreversibly, producing both regioisomers. Regioconvergence towards the final product is ensured by 1,2-migration of the trialkylsilyl group following *β*-bromide elimination.

5. Experimental Section

General procedure for palladium catalyzed *meta*-selective C–H alkynylation of arene: A clean, oven-dried screw cap reaction tube with previously placed magnetic stir-bar was charged with sulfonate ester (0.1 mmol, 1 equiv.), $Pd(OAc)_2$ (10 mol%), Ac-Gly-OH (20 mol%), AgOAc (2 *equiv.*), $Cu(OAc)_2$ (2 *equiv.*). It was then followed by addition of (bromoethynyl)triisopropylsilane (2.5 *equiv.*) and 1,4-dioxane (1 mL). The reaction mixture was vigorously stirred in a preheated oil bath at 80 °C for 24 h. After stipulated time, the reaction mixture was cooled to room temperature and filtered through a celite bed using ethyl acetate as the eluent (30 mL). The filtrate was concentrated and the crude reaction mixture was purified by column chromatography using silica gel (100-200 mesh size) and petroleum-ether / ethyl acetate as the eluent.

Corresponding Authors.

*dmaiti@iitb.ac.in (Prof. Debabrata Maiti)
*robert.paton@chem.ox.ac.uk (Prof. Robert S. Paton)
*srgnchem@gmail.com (Dr. Srimanta Guin)

Author Contributions. S. P. and X. Z. contributed equally to this work

Acknowledgements. We are thankful to SERB-India (CRG/2018/003951) for financial support. Funding from A*STAR Singapore (X.Z.) is gratefully acknowledged. X.Z. and R.S.P. acknowledge the EPSRC Centre for Doctoral Training in Theory and Modelling in Chemical Sciences (EP/L015722/1) and the use of Dirac cluster. R.S.P. acknowledges computational resources from the RMACC Summit supercomputer supported by the National Science Foundation

(ACI-1532235 and ACI-1532236), the University of Colorado Boulder and Colorado State University, and the Extreme Science and Engineering Discovery Environment (XSEDE) through allocation TG-CHE180056. XSEDE is supported by the National Science Foundation (ACI-1548562).

Supporting Information Available. Experimental procedures, analytical data (^{1}H, ^{13}C NMR, MS), computational methodologies, raw atomic values of optimized structures are available in the Supporting Information. Cartesian coordinates (*.xyz* format) for all stationary points are deposited online at DOI:10.5281/zenodo.3376707). This material is available free of charge *via* the internet at http://pubs.acs.org

References

1. For selected references on C–H functionalizations, see: a) Yu, J.-Q.; Shi, Z. *C–H Activation* Vol. 26, Topics in Current Chemistry, Springer: New York, 2010. b) Ribas, X. *C–H and C–X Bond Function: Transition Metal Mediation*: RSC Publishing: London, 2013. c) Kapdi, A.; Maiti, D. *Strategies for Palladium-Catalyzed Non-directed and Directed C−H Bond Functionalization*: Elsevier: Amsterdam, 2017.

2. For selected publications, see: a) McMurray, L.; O'Hara, F.; Gaunt, M. J. Recent Developments in Natural Product Synthesis using Metal-Catalysed C–H Bond Functionalisation. *Chem. Soc. Rev.* **2011**, *40*, 1885-1898. b) Yamaguchi, J.; Yamaguchi, A. D.; Itami, K. C–H Bond Functionalization: Emerging Synthetic Tools for Natural Products and Pharmaceuticals. *Angew. Chem. Int. Ed.* **2012**, *51*, 8960-9009. c) Abrams, D. J.; Provencher, P. A.; Sorensen, E. J. Recent Applications of C–H Functionalization in Complex Natural Product Synthesis. *Chem. Soc. Rev.* **2018**, *47*, 8925-8967. d)

Liu, Y.; Ge. H. Site-selective C–H Arylation of Primary Aliphatic Amines Enabled by a Catalytic Transient Directing Group. *Nat. Chem.* **2016**, *9*, 26-32.

3. a) Roughley, S. D.; Jordan, A. M. The Medicinal Chemist's Toolbox: An Analysis of Reactions used in the Pursuit of Drug Candidates. *J. Med. Chem.* **2011**, *54*, 3451–3479. b) Barker, A.; Kettle, J. G.; Nowak, T.; Pease, J. E. Expanding Medicinal Chemistry Space. *Drug. Discov. Today* **2013**, *18*, 298-304. c) Boström, J.; Brown, D. G.; Young, R. J.; Keserü, G. M. Expanding the Medicinal Chemistry Synthetic Toolbox. *Nat. Rev. Drug Discov.* **2018**, *17*, 709-727.

4. a) Wencel-Delord, J.; Glorius, F. C–H Bond Activation Enables the Rapid Construction and Late-stage Diversification of Functional Molecules. *Nat. Chem.* **2013**, *5*, 369–375. b) Cernak, T.; Dykstra, K. D.; Tyagarajan, S.; Vachalb, P.; Krskab, S. W. The Medicinal Chemist's Toolbox for Late Stage Functionalization of Drug-like Molecules. *Chem. Soc. Rev.* **2016**, *45*, 546-576. c) Beck, M. B.; Stepan, A. F.; Webb, D. in *Synthetic Methods in Drug Discovery*; Blakemore, C. D.; Doyle, P. M.; Fobian, Y., Eds.; Royal Society of Chemistry: Cambridge, 2016, 1, 274–283.

5. Hann, M. M.; Keserü, G. M. Finding the Sweet Spot: The Role of Nature and Nurture in Medicinal Chemistry. *Nat. Rev. Drug Discov.* **2012**, *11*, 355-365.

6. Busacca, C. A.; Fandrick, D. R.; Song, J. J.; Senanayake, C. H. in *Applications of Transition Metal Catalysis in Drug Discovery and Development: An Industrial Perspective*; Crawley, M. L.; Tost, B. M., Eds.; Wiley: New York, 2012, 1–25.

7. a) Dai, H.-X.; Stepan, A. F.; Plummer, M. S.; Zhang, Y.-H.; Yu, J.-Q. Divergent C–H Functionalizations Directed by Sulfonamide Pharmacophores: Late-stage Diversification as a Tool for Drug Discovery. *J. Am. Chem. Soc.* **2011**, *133*, 7222-7228. b) Simonetti, M.; Cannas, D. M.; Just-Baringo, X.; Vitorica-Yrezabal, I. J.; Larrosa, I. Cyclometallated Ruthenium Catalyst Enables Late-stage Directed Arylation of Pharmaceuticals. *Nat. Chem.* **2018**, *10*, 724-731.

8. For selected reviews and publications on distal C(sp^2)–H functionalizations, see; a) Dey, A.; Sinha, S. K.; Achar, T. K.; Maiti, D. Accessing Remote *meta*- and *para*-C–H Bonds with Covalently Attached Directing Groups. *Angew. Chem. Int. Ed.* **2019**, *58*, 10820-10843. b) Wang, J.; Dong, G. Palladium/Norbornene Cooperative Catalysis. *Chem. Rev.* **2019**, *119*, 7478-7528. c) Leitch, J. A.; Frost. C. G. Ruthenium-Catalysed σ-Activation for Remote *meta*-Selective C–H Functionalisation. *Chem. Soc. Rev.* **2017**, *46*, 7145-7153. d) Mihai, M. T.; Genov, G. R.; Phipps, R. J. Access to the *meta* Position of Arenes through Transition Metal Catalysed C–H Bond Functionalisation: A Focus on Metals other than Palladium. *Chem. Soc. Rev.* **2018**, *47*, 149-171. e) Leow, D.; Li, G.; Mei, T.-S.; Yu, J.-Q. Activation of Remote *meta*-C–H Bonds Assisted by an End-on Template. *Nature* **2012**, *486*, 518-522. f) Tobisu, M.; Chatani, N. Remote Control by Steric Effects. *Science* **2014**, *343*, 850-851. g) Davis, H. J.; Mihai, M. T.; Phipps, R. J. Ion Pair-directed Regiocontrol in Transition-metal Catalysis: a *meta*-Selective C–H Borylation of Aromatic Quaternary Ammonium Salts. *J. Am. Chem. Soc.* **2016**, *138*, 12759-12762. h) Ruan, Z.; Zhang, S.-K.; Zhu, C.; Ruth, P. N.; Stalke, D.; Ackermann, L. Ruthenium(II)-catalyzed *meta* C−H Mono- and Difluoromethylations by Phosphine/Carboxylate Cooperation. *Angew. Chem. Int. Ed.* **2017**, *56*, 2045-2049. i) Bag, S.; Patra, T.; Modak, A.; Deb, A.; Maity, S.; Dutta, U.; Dey, A.; Kancherla, R.; Maji, A.; Hazra, A.; Bera, M.; Maiti, D. Remote *para*-C–H Functionalization of Arenes by a D-shaped Biphenyl Template-based Assembly. *J. Am. Chem. Soc.* **2015**, *137*, 11888-11891. j) Okumura, S.; Tang, S.; Saito, T.; Semba, K.; Sakaki, S.; Nakao, Y. *para*-Selective Alkylation of Benzamides and Aromatic Ketones by Cooperative Nickel/Aluminum Catalysis. *J. Am. Chem. Soc.* **2016**, *138*, 14699-14704. k) Hoque, M. E.; Bisht, R.; Haldar, C.; Chattopadhyay, B. Noncovalent Interactions in Ir-Catalyzed C−H Activation: L-Shaped Ligand for *Para*-Selective Borylation of Aromatic Esters. *J. Am. Chem. Soc.* **2017**, *139*, 7745-7748. l) Mihai, M. T.; Williams,

B. D.; Phipps. R. J. *Para*-Selective C–H Borylation of Common Arene Building Blocks Enabled by Ion-Pairing with a Bulky Countercation. *J. Am. Chem. Soc.* **2019***, 141*, 15477-15482. m) Bastidas, J. R. M.; Oleskey, T. J.; Miller, S. L.; Smith, M. R.; Maleczka, R. E. *Para*-Selective, Iridium-Catalyzed C−H Borylations of Sulfated Phenols, Benzyl Alcohols, and Anilines Directed by Ion-Pair Electrostatic Interactions. *J. Am. Chem. Soc.* **2019***, 141*, 15483-15487.

9. a) Brown, D. G.; Boström, J. Analysis of Past and Present Synthetic Methodologies on Medicinal Chemistry: Where have all the New Reactions Gone? *J. Med. Chem.* **2016**, *59*, 4443-4458. b) Leeson, P. D.; Springthorpe, B. The Influence of Drug-like Concepts on Decision-making in Medicinal Chemistry. *Nat. Rev. Drug Discov.* **2007**, *6*, 881-890. c) Nadin, A.; Hattotuwagama, C.; Churcher, I. Lead-oriented Synthesis: A New Opportunity for Synthetic Chemistry. *Angew. Chem. Int. Ed.* **2012**, *51*, 1114–1122.

10. a) Fosgerau, K.; Hoffmann, T. Peptide Therapeutics: Current Status and Future Directions. *Drug Discov. Today* **2015**, *20*, 122-128. b) Liu, T.; Qiao, J. X.; Poss, M. A.; Yu, J.-Q. Palladium(II)-Catalyzed Site-Selective C(sp3)−H Alkynylation of Oligopeptides: A Linchpin Approach for Oligopeptide–Drug Conjugation. *Angew. Chem. Int. Ed.* **2017**, *56*, 10924-10927.

11. Trofimov, B. A.; Stepanova, Z. V.; Sobenina, L. N.; Mikhaleva, A. I.; Ushakov, I. A. Ethynylation of Pyrroles with 1-Acyl-2-bromoacetylenes on Alumina: A Formal "Inverse Sonogashira Coupling." *Tetrahedron Lett.* **2004**, *45*, 6513-6516.

12. Diederich, F.; Stang, P. J.; Tykwinski, R. R. *Acetylene Chemistry: Chemistry, Biology and Material Science*: Wiley-VCH: Weinheim, Germany, 2005.

13. For selected publications on *ortho*-alkynylation, see: a) Tobisu, M.; Ano, Y.; Chatani, N. Palladium-catalyzed Direct Alkynylation of C–H Bonds in Benzenes. *Org. Lett.* **2009**, *11*, 3250-3252. b) Viart, H. M.-F., Bachmann, A., Kayitare, W. & Sarpong, R. *β*-Carboline Amides as

Intrinsic Directing Groups for C(sp^2)−H Functionalization. *J. Am. Chem. Soc.* **2017**, *139*, 1325-1329. c) Ruan, Z.; Sauermann, N.; Manoni, E.; Ackermann, L. Manganese-catalyzed C–H Alkynylation: Expedient Peptide Synthesis and Modification. *Angew. Chem. Int. Ed.* **2017**, *56*, 3172-3176. d) Tan, E.; Quinonero, O.; de Orbe, M. E.; Echavarren, A. M. Broad-scope Rh-Catalyzed Inverse-Sonogashira Reaction Directed by Weakly Coordinating Groups. *ACS Catal.* **2018**, *8*, 2166-2172.

14. A *meta*-selective alkynylation was achieved using Catellani approach, however substrate scope was limited to silyl acetylenic derivatives. Wang, P.; Li, G.-C.; Jain, P.; Farmer, M. E.; He, J.; Shen, P.-X.; Yu, J.-Q. Ligand-promoted *meta*-C−H Amination and Alkynylation. *J. Am. Chem. Soc.* **2016**, *138*, 14092-14099.

15. For publications on *para*-alkynylation, see: a) de Haro, T.; Nevado, C. Gold-Catalyzed Ethynylation of Arenes. *J. Am. Chem. Soc.* **2010**, *132*, 1512-1513. b) Brand, J. P.; Waser, J. *Para*-selective Gold-catalyzed Direct Alkynylation of Anilines. *Org. Lett.* **2012**, *14*, 744-747.

16. a) Bag, S.; Jayarajan, R.; Mondal, R.; Maiti, D. Template-assisted *meta*-C−H Alkylation and Alkenylation of Arenes. *Angew. Chem. Int. Ed.* **2017**, *56*, 3182-3186. b). Bag, S.; Jayarajan, R.; Dutta, U.; Chowdhury, R.; Mondal, R.; Maiti, D. Remote *meta*-C–H Cyanation of Arenes Enabled by a Pyrimidine-based Auxiliary. *Angew. Chem. Int. Ed.* **2017**, *56*, 12538-12542. c) Achar, T. K.; Zhang X.; Mondal, R.; Shanavas, M, S.; Maiti, S.; Maity, S.; Pal, N.; Paton, R. S.; Maiti, D. Palladium-catalyzed Directed *meta*-Selective C−H Allylation of Arenes: Unactivated Internal Olefins as Allyl Surrogates. *Angew. Chem. Int. Ed.* **2019**, *58*, 10353-10360.

17. a) Negishi, E.; Anastasia, A. Palladium-catalyzed Alkynylation. *Chem. Rev.* **2003**, *103*, 1979-2017. b) Caspers, L. D.; Nachtsheim, B. J. Directing-Group-mediated C–H-Alkynylations. *Chem. Asian J.* **2018**, *13*, 1231-1247.

18. Sinha, S. K.; Bhattacharya, T.; Maiti, D. Role of Hexafluoroisopropanol in C–H Activation. *React. Chem. Eng.* **2019**, *4*, 244-253.

19. Reddy, D. S.; Jian, K. The Testosterone-derived Neurosteroidandrostanediol is a Positive Allosteric Modulator of GABAA Receptors. *J. Pharmacol. Exp. Ther*. **2010**, *334*, 1031-1041.

20. Kuhl, H. Pharmacology of Estrogens and Progestogens: Influence of Different Routes of Administration. *Climacteric*. **2005**, *8*, 3-63.

21. Gaussian 16, Revision A.01. Frisch, M. J.; Trucks, G. W.; Schlegel, H. B.; Scuseria, G. E.; Robb, M. A.; Cheeseman, J. R.; Scalmani, G.; Barone, V.; Petersson, G. A.; Nakatsuji, H.; Li, X.; Caricato, M.; Marenich, A. V.; Bloino, J.; Janesko, B. G.; Gomperts, R.; Mennucci, B.; Hratchian, H. P.; Ortiz, J. V.; Izmaylov, A. F.; Sonnenberg, J. L.; Williams-Young, D.; Ding, F.; Lipparini, F.; Egidi, F.; Goings, J.; Peng, B.; Petrone, A.; Henderson, T.; Ranasinghe, D.; Zakrzewski, V. G.; Gao, J.; Rega, N.; Zheng, G.; Liang, W.; Hada, M.; Ehara, M.; Toyota, K.; Fukuda, R.; Hasegawa, J.; Ishida, M.; Nakajima, T.; Honda, Y.; Kitao, O.; Nakai, H.; Vreven, T.; Throssell, K.; Montgomery, J. A., Jr.; Peralta, J. E.; Ogliaro, F.; Bearpark, M. J.; Heyd, J. J.; Brothers, E. N.; Kudin, K. N.; Staroverov, V. N.; Keith, T. A.; Kobayashi, R.; Normand, J.; Raghavachari, K.; Rendell, A. P.; Burant, J. C.; Iyengar, S. S.; Tomasi, J.; Cossi, M.; Millam, J. M.; Klene, M.; Adamo, C.; Cammi, R.; Ochterski, J. W.; Martin, R. L.; Morokuma, K.; Farkas, O.; Foresman, J. B.; Fox, D. J. Gaussian, Inc., Wallingford CT, **2016**.

22. Chen, G.; Gong, W.; Zhuang, Z.; Andrä, M. S.; Chen, Y. Q.; Hong, X.; Yang, Y. F.; Liu, T.; Houk, K. N.; Yu, J. Q. Ligand-accelerated Enantioselective Methylene C(sp^3)–H Bond Activation. *Science* **2016**, *353*, 1023-1027.

23. Cheng, G. J.; Yang, Y. F.; Liu, P.; Chen, P.; Sun, T. Y.; Li, G.; Zhang, X.; Houk, K. N.; Yu, J. Q.; Wu, Y. D. Role of *N*-Acyl Amino Acid Ligands in Pd(II)-Catalyzed Remote C–H Activation

of Tethered Arenes. *J. Am. Chem. Soc.* **2014**, *136*, 894-897.

24. Yang, Y. F.; Hong, X.; Yu, J. Q.; Houk, K. N. Experimental-Computational Synergy for Selective Pd(II)-Catalyzed C–H Activation of Aryl and Alkyl Groups. *Acc. Chem. Res.* **2017**, *50*, 2853-2860.

25. Dutta, U.; Modak, A.; Bhaskararao, B.; Bera, M.; Bag, S.; Mondal, A.; Lupton, D. W.; Sunoj, R. B.; Maiti, D. Catalytic Arene *meta*-C–H Functionalization Exploiting a Quinoline-based Template. *ACS Catal.* **2017**, *7*, 3162-3168.

26. Kozuch, S.; Shaik, S. How to Conceptualize Catalytic Cycles? The Energetic Span Model. *Acc. Chem. Res.* **2011**, *44*, 101-110.

27. Yang, Y. F.; Cheng, G. J.; Liu, P.; Leow, D.; Sun, T. Y.; Chen, P.; Zhang, X.; Yu, J. Q.; Wu, Y. D.; Houk, K. N. Palladium-catalyzed *meta*-Selective C–H Bond Activation with a Nitrile-containing Template: Computational Study on Mechanism and Origins of Selectivity. *J. Am. Chem. Soc.* **2014**, *136*, 344-355.

28. Anand, M.; Sunoj, R. B.; Schaefer, H. F. Non-innocent Additives in a Palladium(II)-catalyzed C–H Bond Activation Reaction: Insights into Multimetallic Active Catalysts. *J. Am. Chem. Soc.* **2014**, *136*, 5535-5538.

29. Guin, S.; Dolui, P.; Zhang, X.; Paul, S.; Singh, V. K.; Pradhan, S.; Chandrashekar, H. B.; Anjana, S. S.; Paton, R. S.; Maiti, D. Iterative Arylation of Amino Acids and Aliphatic Amines via δ-C(sp^3)−H Activation: Experimental and Computational Exploration. *Angew. Chem. Int. Ed.* **2019**, *58*, 5633-5638.

30. 30. Usui, K.; Haines, B. E.; Musaev, D. G.; Sarpong, R. Understanding Regiodivergence in a Pd(II)-Mediated Site-Selective C-H Alkynylation. *ACS Catal.* **2018**, *8*, 4516-4527.

31. Danheiser, R. L.; Kwasigroch, C. A.; Tsai, Y. M. Application of Allenylsilanes in [3+2]

Annulation Approaches to Oxygen and Nitrogen Heterocycles. *J. Am. Chem. Soc.* **1985**, *107*, 7233-7235.

32. Kanno, H.; Nakamura, K.; Noguchi, K.; Shibata, Y.; Tanaka, K. Rhodium-Catalyzed Cycloisomerization of 2-Silylethynyl Phenols and Anilines via 1,2-Silicon Migration. *Org. Lett.* **2016**, *18*, 1654-1657.

33. Dudnik, A. S.; Xia, Y.; Li, Y.; Gevorgyan, V. Computation-Guided Development of Au-Catalyzed Cycloisomerizations Proceeding via 1,2-Si or 1,2-H Migrations: Regiodivergent Synthesis of Silylfurans. *J. Am. Chem. Soc.* **2010**, *132*, 7645-7655.

34. Li, T.; Zhang, L. Bifunctional Biphenyl-2-Ylphosphine Ligand Enables Tandem Gold-Catalyzed Propargylation of Aldehyde and Unexpected Cycloisomerization. *J. Am. Chem. Soc.* **2018**, *140*, 17439-17443.

35. Taguchi, H.; Miyashita, H.; Tsubouchi, A.; Takeda, T. First Anionic Ailyl Migration from sp^2 Carbon to Carbonyl Oxygen. Stereospecific Allylation of (Z)-β-Trimethylsilyl-α,β-Unsaturated Ketones. *Chem. Commun.* **2002**, *2*, 2218-2219.

36. Tsubouchi, A.; Sasaki, N.; Enatsu, S.; Takeda, T. Regio- and Stereoselective Preparation of (Z)-Silyl Enol Ethers by Three-component Coupling using α,β-Unsaturated Acylsilanes as Core Building Blocks. *Tetrahedron Lett.* **2013**, *54*, 1264-1267.

37. Tsubouchi, A.; Matsuda, H.; Kira, T.; Takeda, T. Silyl Migration in Conjunction with Substitution on Silicon in Copper(I) t-Butoxide-promoted Coupling between o-Silylphenyl Ketones and Organic Halides. *Chem. Lett.* **2009**, *38*, 1180-1181.

TOC GRAPHIC

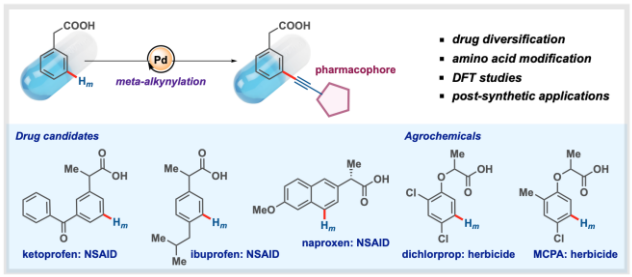
COOH
Pd
meta-alkynylation
COOH
pharmacophore
drug diversification
amino acid modification
DFT studies
post-synthetic applications
Drug candidates
Agrochemicals
ketoprofen: NSAID
ibuprofen: NSAID
naproxen: NSAID
dichlorprop: herbicide
MCPA: herbicide